Analytical Methods

rsc.li/methods

ROYAL SOCIETY
OF **CHEMISTRY**

PAPER
Petra van der Merwe and Patricia Forbes
Comparison of three sorbents for thin film solid phase
microextraction of haloacetic acids from water

Indexed in Medline!

Check for updates

Comparison of three sorbents for thin film solid phase microextraction of haloacetic acids from water†

Petra van der Merwe [ID] and Patricia Forbes [ID] *

Water disinfection inevitably leads to disinfection byproduct formation, such as haloacetic acids. Many disinfection byproducts reportedly have adverse health effects and, in many instances, including four haloacetic acids, are classified as potential carcinogens. As the global awareness of these compounds increases, more regulatory bodies include certain disinfection byproduct groups in their regulations. Rugged, fast, and cheap analytical quantification methods are therefore crucial. In this paper, a thin film extraction method for haloacetic acids is outlined. Thin films were synthesized in-house using a spin coating procedure, which allowed for easy adjustment of the sorbent choice and film geometry. PDMS, Carboxen®, and HLB were of interest and their extraction potential for HAAs from spiked water was tested in three film variations. PDMS films impregnated with HLB or Carboxen® improved the extraction drastically compared to PDMS films. Specifically, HLB impregnated films achieved excellent extraction efficiencies for tri-substituted analytes (51% for BDCAA, 77% for CDBAA, and 92% TBAA), which are often present at extremely low concentrations in water. In addition to the extraction experiment, a computational model was applied to compare PDMS and HLB. Trends observed in the computational data reflected in the experimental results, showing the validity of the model and confirming that physisorption through hydrogen bonding was mainly responsible for successful extraction.

Introduction

Disinfection has become an indispensable step in the modern water treatment process. However, disinfection comes with the ramification of disinfection byproduct (DBP) formation. To date, over 700 DBPs have been identified, of which many pose adverse health effects to humans.[1] Yet only a few are being regulated in drinking water guidelines at an international[2] or local level.[3–9] Trihalomethanes (THMs) were the first DBPs discovered[10] and along with haloacetic acids (HAAs) are the most prevalent DBPs, especially when water chlorination or chloramination processes are implemented.[11] THMs have been included in many drinking water guidelines since the late 1990s, whilst select HAAs were only included in some;[3,5,8] however, they have been increasingly added during updates since 2010.[2,4,6,7] Typically, five HAAs (HAA5), namely monochloroacetic acid (MCAA), dichloroacetic acid (DCAA), trichloroacetic acid (TCAA), monobromoacetic acid (MBAA), and DBAA (dibromoacetic acid), are regulated, whereas nine HAAs (HAA9) are frequently encountered (HAA5 plus tribromoacetic acid (TBAA), bromochloroacetic acid (BCAA),

bromodichloroacetic acid (BDCAA), and chlorodibromoacetic acid (CDBAA)).[12] Increased awareness and inclusion in drinking water guidelines have escalated the need for sensitive, environmentally conscious, fast, and cost-effective analytical methods for HAAs in treated water.

HAAs are small, polar compounds with low pK_a values (0.03–2.89) and high boiling points (all above 185 °C),[13] complicating extraction and analysis. Initial analytical methods were mostly gas chromatography (GC) based,[14–16] thus requiring an extraction step from the water matrix into an organic solvent and derivatization to nonpolar variants, as direct injection onto GC columns would be detrimental.[17] All versions of the commonly implemented United States Environmental Protection Agency (US EPA) Method 552 series follow this pattern, utilizing varying extraction techniques and derivatization agents prior to GC-ECD analysis.[18–21] In version 552.3, which has become a globally accepted routine method, liquid–liquid extraction (LLE) is followed by Fischer esterification to produce the methyl esters of HAAs.[21] Despite being a common method, it is time-intensive, applies harsh chemicals (such as sulfuric acid), and produces considerable amounts of laboratory waste. Thus, numerous methods attempting to simplify analysis and save time have been outlined in the literature over the past 20 years.[22–29]

Especially ion chromatography (IC, such as in EPA Method 557 (ref. 30)) and liquid chromatography (LC) based methods

Department of Chemistry, Faculty of Natural and Agricultural Sciences, University of Pretoria, South Africa. E-mail: patricia.forbes@up.ac.za

† Electronic supplementary information (ESI) available. See DOI: https://doi.org/10.1039/d4ay00634h

have progressively become more prominent, as they allow for direct injection.[31–40] Regardless, many laboratories, especially in developing countries, do not have access to these types of instruments and rely on the available GC equipment. Additionally, many LC-based methods do not reach the sensitivities required to detect HAAs at low $\mu g\,L^{-1}$ (ppb) levels in water.[40,41] Hence, there is a need to develop GC-based methods that simplify extraction and derivatization steps, using a 'green' approach.

In the pursuit of making methods more environmentally friendly, reducing solvent and material usage has become imperative. Therefore, miniaturized extraction methods, such as single drop microextraction,[28] hollow fiber membrane liquid-phase microextraction,[42] and headspace solid-phase micro-extraction (HS-SPME),[22,23] have been reported. Although these methods may achieve good detection limits, key disadvantages are reported, such as the elevated temperature required to volatilize heat labile analytes, which might lead to analyte losses. Another microextraction technique that has garnered attention since its inception is thin film solid phase micro-extraction (TF-SPME).[43,44] In this adaptation of solid phase microextraction (SPME), a thin film or membrane acts as the solid phase and is either used in headspace or direct applications for volatile organic compounds (VOCs), semi-volatile organic compounds (SVOCs) and very volatile organic compounds (VVOCs).[45,46] The increased surface to volume ratio, compared to other SPME methods, enhances extraction efficiency and sensitivity.[44,45] Additionally, TF-SPME allows for on-site sampling[47] and introduces opportunities for innovative geometries, such as vial-coated or blade coated TF-SPME.[44] Previous applications of TF-SPME include various sample matrices, spanning from diverse environmental and food samples to biological fluids.[44] The most prominent work on TF-SPME stems from the Pawliszyn group, which has described multiple thin film applications, where desorption occurred in thermal desorption units (TDUs) with direct injection into the GC inlet.[47–49]

The ease-of-use of TF-SPME makes it an ideal method for HAA analysis in water, since it introduces flexibility into the extraction process, allowing it to be performed both on-site or at any point within the preparation method. The order of extraction and derivatization becomes adjustable, which is extended to the desorption, since both back-extraction and thermal desorption are reasonable possibilities. Therefore, TF-SPME may be used as a faster, greener alternative to current GC-based HAA analysis methods or may be used as a pre-concentration step in LC applications to increase the sensitivity of these methods. Furthermore, the improved sorbent to volume ratio[44] of the extraction device may address the issue of poor sensitivity, often reported for brominated and tri-substituted analytes.[25,31,32,35,50] Additionally, various sorbent types and combinations can be explored to further increase sensitivity and/or selectivity. In this paper, a facile method is outlined to synthesize polydimethylsiloxane (PDMS) thin films, using a spin-coating technique, which allows for easy incorporation of a variety of sorbents into the thin films. The extraction potential of PDMS films for HAAs is compared to that of films impregnated with Carboxen® or hydrophilic-lipophilic balance (HLB) particles. Three film types of each sorbent were compared, and experimental extraction efficiencies for HAAs were contrasted to the computationally determined binding energies of the sorbent and the analyte for the first time. Computational data furthermore provided information on a molecular level of the nature of the sorptive processes and interactions taking place.

Experimental

Chemicals and materials

A HAA standard mix (2000 $\mu g\,mL^{-1}$ in methyl-*tert*-butyl-ether (MtBE), >98% purity) and the surrogate, 2-bromobutanoic acid (99.3%) were purchased from Sigma-Aldrich, whilst the internal standard (IS), 1,2,3-trichloropropane (99.3% pure), was obtained from Supelco (both brands associated with Merck KGaA, Hessen, Germany). Individual standards for BCAA (1000 $\mu g\,mL^{-1}$, 97%), BDCAA (40 $\mu g\,mL^{-1}$, 98.8%), CDBAA (100 $\mu g\,mL^{-1}$, 97%), DBAA (1000 $\mu g\,mL^{-1}$, 90%), DCAA (1000 $\mu g\,mL^{-1}$, 99.2%), MBAA (40 $\mu g\,mL^{-1}$, 100%), MCAA (60 $\mu g\,mL^{-1}$, 99%), and TCAA (1000 $\mu g\,mL^{-1}$, 100%), all in MtBE, were bought from Separations (Pty) Ltd (Gauteng, South Africa), which supplies AccuStandard (AccuStandard Inc., Connecticut, United States).

HPLC/GC-grade MtBE was ordered from Sigma-Aldrich (Pty) Ltd (Merck KGaA, Hessen, Germany), and anhydrous, HPLC-grade methanol (MeOH) from Radchem (Pty) Ltd (Gauteng, South Africa), which supplies Macron chemicals, an Avantor brand (Pennsylvania, United States). ACS-grade H_2SO_4, $NaHCO_3$, and anhydrous granulated Na_2SO_4 were supplied by Associated Chemical Enterprises (ACE) (Pty) Ltd (Gauteng, South Africa). Ultrapure water was collected from a PURELAB® Chorus 1 Complete water purification system (max conductivity, <2000 $\mu S\,cm^{-3}$, ELGA LabWater, Illinois, United States). Analytical grade acetone and isopropyl alcohol were purchased from Stargate Scientific (Gauteng, South Africa) and Radchem (Pty) Ltd (Gauteng, South Africa), respectively.

Polyacrylic acid (25% PAA) sodium salt solution in water was purchased from Sigma-Aldrich (Merck KGaA, Hessen, Germany) as a sacrificial layer for thin film synthesis. The two-part PDMS elastomer kit, Sylgard 184 Elastomer, was ordered through Elvesys S.A.S (Île-de-France, France) from Dow Inc. (Michigan, United States). HLB particles were removed from Oasis® HLB 3cc/60 mg SPE cartridges (Waters Corporation, Massachusetts, US) and Carboxen® 569, 20/45 mesh, was purchased from Supelco (Merck KGaA, Hessen, Germany).

Methods

Synthesis of thin films. Thin films were synthesized, using a spin-coating procedure, utilizing a Laurell Technologies Corporation WS-650MZ-23NPPB spin coater (Elvesys S.A.S, Île-de-France, France). PDMS and the curing agent were mixed in a 10 : 1 ratio and were degassed in a vacuum chamber. A glass substrate (60 mm × 60 mm) was cleaned with distilled water, acetone and IPA. This was followed by two additional rinses with acetone and IPA only and drying using pressurized air. PAA

(2 mL, 25%) was added to the substrate on the spin coater chuck and spun for a total time of 15 s at an acceleration of 150 rpm s^{-1} and a maximum speed of 1000 rpm. The layer was cured at 150 °C for 5 min on a hot plate. After cooling, 2 mL PDMS was added dropwise onto a slide and spun for 30 s at 100 rpm s^{-1} at a maximum speed of 300 rpm. This step was repeated five times and then the film was cured on a hot plate for 30 min at 80 °C. Thicker sides, necessary for submersion and handling, were created by pipetting lines of PDMS along two opposite edges of the film and curing for an additional 30 min. The film edges were carefully cut from the glass slide with a scalpel and then submerged in a water bath and sonicated for 30 min. After allowing all water to evaporate, the film was carefully lifted off the substrate and stored in a Petri dish, sealed with Parafilm M® until use. Prior to characterization and use, films were cut into six pieces (10 mm × 60 mm), of which two were used for characterization and three for the extraction potential study.

Three variants of sorbent-impregnated thin films were prepared for each sorbent type. Two variants contained differing amounts of sorbent (Carboxen®: 0.5 and 2.4 g; HLB: 0.2 and 1.1 g) mixed into the PDMS prior to degassing, and one with the sorbent (Carboxen®: 1.2 g; HLB 0.5 g) added to the film surface during the curing process. Carboxen® particles were ground with a pestle and mortar prior to addition to the PDMS or film.

Determination of thin film extraction potential by analysis of residual HAA concentrations after thin film extraction using EPA Method 552.3. Two controls were prepared to account for any analyte changes due to the extraction process: one was prepared and immediately stored (−4 °C, labelled EPA), while the other was treated identically to the standards used in the extraction experiments (labelled EPA_ON). The two control types, extraction standards for extraction with PDMS, and three film types of each sorbent were prepared in triplicate.

Each control or standard was prepared by spiking distilled water (40 mL) with a surrogate (20.3 μg mL^{-1} in MtBE), and a mixed HAA standard (8 μg mL^{-1} daily stock in MeOH) in 50 mL glass bottles with PTFE lined caps (Stargate Scientific, Gauteng, South Africa). H$_2$SO$_4$ (2 mL) was added, followed by conditioned films (10 mm × 60 mm, sonicated for 30 min in distilled water and left in distilled water for 5 min directly prior to use), and inert stirrer bars. Stirring was set to 100 rpm for 24 hours at room temperature in the closed bottles. After this extraction step, the thin films were removed. Any HAAs remaining in solution after TFSPME were derivatized by adding

14 g Na$_2$SO$_4$ and 4 mL extraction solvent (1 mg L^{-1} IS in MtBE) to the vials, which were then shaken for 3 min, followed by 5 min phase separation. 3 mL organic layer was removed with a Pasteur pipette into 15 mL conical centrifuge tubes, to which 3 mL 10% H$_2$SO$_4$ in MeOH was added. The mixture was placed in a water bath at 50 °C for 2 hours. A washing step (7 mL of 150 g L^{-1} Na$_2$SO$_4$ in distilled water), removal of the aqueous layer, and a neutralization step (1 mL saturated NaHCO$_3$ solution) followed the derivatization. 1.5 mL organic layer was transferred into a 2 mL amber autosampler vial and stored in a freezer (−18 °C) until analysis (Fig. 1).

Analytical instrumentation. Analysis was performed with an Agilent 6890 GC-ECD system (Agilent, California, US), equipped with an autosampler (Agilent, 7683 series) and a Restek Rsi-5Sil MS capillary column (30 m × 0.25 mm × 0.25 μm df) (Restek, Pennsylvania, US) with an Integra-Guard. After syringe pre-washes with MtBE, a 3 μL sample was injected in splitless mode at 200 °C. Ultra-high purity grade helium (Afrox, Gauteng, South Africa) was used as carrier gas at a constant flow rate of 1 mL min^{-1}. The initial temperature was set to 35 °C (hold 10 min) and then was ramped to 75 °C at 5 °C min^{-1} (hold 15 min), ramped again to 100 °C at 5 °C min^{-1} (hold 1 min), and lastly increased to 220 °C at 25 °C min^{-1} (hold 1 min) (method adapted from Xie[51]). The detector heater was set to 300 °C, the anode flow to 6 mL min^{-1}, the makeup gas, nitrogen (Air Products Pty Ltd, Gauteng, South Africa), was set to a flow rate of 30 mL min^{-1} and the electrometer was set to 188.5 × 5 Hz. Data were analysed and processed with ChemStation software (Agilent, California, US). Analyte peaks were identified and confirmed using a combination of individual standards and retention times determined by GC-mass spectrometry (MS) (Agilent 7890A GC, with an Agilent 5957 inert MSD (California, US)), using the same conditions and chromatographic criteria.

Characterization

Sorbent particles were analysed with a Zeiss Gemini Ultra Plus FEG (Carl Zeiss AG, Baden-Wuertemberg, Germany) in scanning electron microscopy (SEM) mode (2 kV) and thin films were characterized using a Zeiss Axio Imager.A1m microscope (Carl Zeiss AG, Baden-Wuertemberg, Germany). The films were cut into squares and placed on glass microscope slides for analysis, whilst sorbent particles were stuck on carbon tape attached to an aluminium stub and coated with carbon using a Quorum Q150 S/E/ES Sputter Coating Unit (Quorum Technologies, East
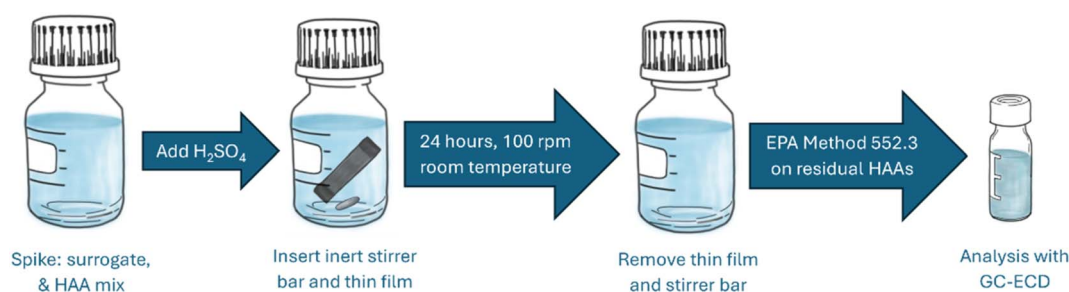

Fig. 1 Flow chart of the experimental procedure used to compare thin film extraction efficiency.

Sussex, United Kingdom). The results were further evaluated, based on particle size and spread, and classified according to the relation of the area visibly covered by sorbent particles at a certain depth of field and the area of a given square (termed coverage), using ImageJ.[52]

The film thickness was determined by placing the films on the edge of a glass microscope slide, which was then inserted into a clamp in an upright position so that the edge of the slide and film pointed towards the objective lens. Average film thicknesses were determined from the micrographs taken using ImageJ.[52]

Additionally, FTIR and BET analyses were employed for thin film characterisation. For the former, a JASCO FT/IR-4X was used (JASCO Inc., Maryland, US), whilst an Autosorb iQ adsorption analyser was used for BET analysis (Anton Paar QuantaTec. Inc., Florida, US). The thin films were cut into smaller squares (10 mm × 10 mm) and placed into dried BET cells, followed by degassing for 10 hours at 120 °C. Analysis was done using nitrogen at 77 K, and data were analysed with Quantochrome® ASiQwin™ software (Anton Paar QuantaTec. Inc., Florida, US).

Data processing

Chromatographic peak area ratios were calculated by dividing analyte peak areas with the IS peak area. The standard deviations and percent relative standard deviations (% RSDs) of triplicate measurements were calculated from these peak area ratios. In the cases where the % RSD exceeded 15%, the z-scores were calculated to test for outliers. z-Scores exceeding an absolute value of one were treated as outliers, given that they are one standard deviation away from the mean. The relative extraction potential was calculated using:

$$\% \text{ rel. ext.} = \frac{(\text{area(cont.)} - \text{area(ext.)})}{\text{area(cont.)}} \times 100$$

where % rel. ext. stands for the percent relative extraction, area(cont.) stands for the peak area ratios of the control of interest, and area(ext.) for the peak area ratio of the residual after extraction. Single factor analysis of variance (ANOVA) was used to test the statistical significance of differences observed between the means of relative extraction achieved for different film types, sorbents and both controls in separate tests. The null hypothesis was stated as follows: H_0: $\mu = 0$, indicating that the means of the groups of interest were equal, and it was tested at a 95% confidence level, with 0.05 as the critical value. The alternative hypothesis was stated as $H_1 \neq 0$, indicating that the means between the groups of interest differed significantly.

Computational study

HAA9 and two sorbents (HLB and PDMS) were modelled and interfaced to determine binding energies. Given that the structure of Carboxen® is proprietary, no suitable molecular models for comparison could be constructed. The geometries of the sorbents and analytes were optimized using Density Functional Theory (DFT), using the B3LYP functional and 6-311G++(d,p) basis set and the Polarizable Continuum Model

(PCM)[53] to implicitly model water as a solvent. All optimization experiments were performed in Gaussian 16, Revision C.01 (ref. 54) and calculation details specified were performed using software-defined default settings. The *XYZ* coordinates of all optimized molecules are included in Tables S1–S3 of the ESI,† which also includes the figures of the resulting interfaces (Fig. S1–S9†). Given that all sorbents of interest were polymers, special considerations using molecular approaches were required during modelling. Sorbents were optimized step-wise, adding a functional group with each iteration and interfacing each with analytes to determine the functional group with the strongest binding potential. Complete, optimized sorbent monomers (Fig. 2) were interfaced with the analytes in proximity to this functional group. Additionally, the effect of the distance between these atoms on the resulting energy was tested by using one exemplary analyte (BCAA) and creating input files where the atoms were 1.2, 1.4, 1.6, 2, and 2.5 Å apart. The resulting energies, for both individual molecules, as well as interfaces, were converted from Hartree to kcal mol^{-1} and tabulated. The binding energies were calculated using:

$$\Delta E_{\text{bind}} = E_{\text{i}} - E_{\text{s}} - E_{\text{a}}$$

where E_{i} is the electronic energy of the optimized sorbent–analyte interface, and E_{s} and E_{a} the electronic energies of the optimized sorbent monomer and analyte, respectively.

Results and discussion

Computational study

Sorbent monomers and analytes were interfaced at varying distances to each other, to test whether the input distance between the two molecules impacted the resulting data. It was found that the binding energies varied only slightly between input distances, demonstrating that all distances were optimized towards the same local minimum.

Furthermore, the binding energies of the two sorbents, HLB and PDMS, were determined. The binding energies of HLB ranged from −8.05 to −11.52 kcal mol^{-1} and those for PDMS ranged from −5.60 to −7.26 kcal mol^{-1} (Fig. 3). For both sorbents the key to the successful interaction appeared to be hydrogen bonds, formed between the hydroxyl group of the analyte and an electronegative atom of the sorbent monomer: in the HLB monomer, the oxygen of the pyrrolidone and in the PDMS monomer, the oxygen of the siloxane. The characteristics of the proposed hydrogen bonds adhered to the definition and criteria outlined by the International Union of Pure and Applied
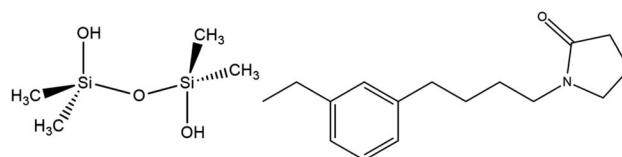

Fig. 2 Structural formulae of the PDMS (left) and HLB monomers (right).
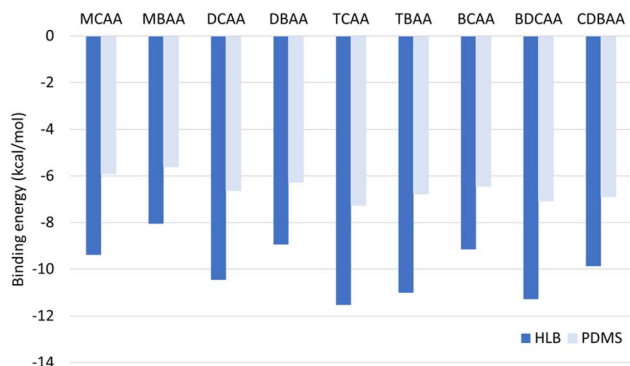
Fig. 3 Computationally determined binding energies of the most stable protonated HAA conformers interfaced with a monomer of each sorbent (HLB and PDMS).

Chemistry (IUPAC) for hydrogen bonds.[55] Especially the geometries adhered to the criteria, as hydrogen-bond acceptor (H⋯Y) bonds were linear, with angles close to 180° (criteria E3 (ref. 55) – 173° for HLB and 172° for PDMS), and the bond lengths of the covalent X–H bond increased after hydrogen bond formation (criteria E4,[55] see Table S4†). Moreover, bond lengths and binding energies fell well within the classification of a moderate hydrogen bond according to Grabowski.[56] Based on these results, the extraction of HAA with both sorbents was expected to occur and could be attributed to physisorption, as hydrogen bond formation is the classical indicator of this type of sorption. However, HLB was expected to perform better as a sorbent, given more negative binding energies, implying stronger interactions with the analytes.

Bond geometries further provided information on the observed difference in binding energy between the two sorbents. The shorter bond lengths of the H⋯Y bond (1.47–1.61 Å versus 1.68–1.76 Å for PDMS) in the HLB interface indicate a stronger hydrogen bond.[55] Given that the oxygen of the pyrrolidone is less sterically hindered and more electronegative in its sp^2 form, compared to the oxygen in the siloxane (sp^3), it is to be expected that the binding energy of the PDMS interface is more positive than that of the HLB interface.

Beyond the comparison of the sorbents, trends between analytes were considered. A strong trend correlating the level of halogen substitution and binding energy was observed. In criterion E2 of the IUPAC document on hydrogen bonding, a proportionality between the strength of the H⋯Y bond and the electronegativity of the X atom is described.[55] This furthermore implies a correlation with the degree of polarization of the X–H bond, and since nearby atoms and environmental factors influence bond polarity, the electronegative halogens in proximity to the small HAA molecules should be considered.[56] Hence, it was hypothesized that electronegative halogens in proximity to the X–H bonds influence their polarity and consequently the level of halogen substitution directly impacts the binding energy. This was further supported by the observation that binding energies were more negative for the analytes containing the more electronegative chlorine compared to the bromine. Since the more electronegative atoms increased the

polarity of the X–H bond, the hydrogen bond increased in strength. Based on the computational results, it was expected that HLB impregnated films would perform better than PDMS films and that the more substituted analytes would be extracted to a greater degree.

Characterization

Sorbent particle characterization. SEM imaging of the Carboxen® particles revealed an average particle diameter of 460.6 μm. Their surfaces appeared to be smooth with intermittent small crevices (Fig. 4). A closer inspection of a crevice revealed an irregular morphology beneath the smooth surface (Fig. 4b). These pores and bumps visible within the crevices are likely exposed systems of tapered micropores described by the Carboxen® manufacturer, which increase the range of particle sizes that can be adsorbed.[57] The minute micropore openings are not visible on the undamaged surface; however, they become exposed in the damaged areas of the crevices. Due to their size and density, Carboxen® particles were spun off during thin film synthesis with the spin coater, and therefore needed to be ground, to reduce their size and thus mass. The surfaces of the ground particles had a similar morphology to that observed in the crevices, indicating that grinding the particles had no detrimental effect on the microporosity of the material. Ground particles were not uniform in their size, but on average appeared to be rectangular, almost square in most instances, with an average length and width of 100 μm.

Imaging of HLB particles displayed a similarly smooth surface and an average particle diameter of 26.9 μm. These particles only had dispersed pores on their surfaces, which were smoother overall (Fig. 4d). Given the particle size and powdered nature of HLB, mixing the particles into PDMS posed no obstacle to thin film synthesis and their grinding was not necessary.

Thin film characterization. FTIR analysis confirmed the successful addition of the sorbent materials to all PDMS thin films, as bands absent on the PDMS film were evident on all impregnated films (Fig. S10 in the ESI†). The light micrographs of the PDMS films showed that their surfaces were smooth; however, they easily attracted dust and other particles (Fig. 5). Imaging of sorbent containing thin film variations revealed that the particles for both HLB and Carboxen® were well distributed within the films (Fig. 6). However, due to the size variation of the ground Carboxen®, films containing a lower mass of this material had some aggregation of larger particles, reducing dispersion homogeneity (Fig. 6a). For HLB, the film containing a greater mass of material had some areas with fewer particles; however, generally these areas were equally dispersed (Fig. 6e).

Film 'coverage' was used to describe the ratio of the area visibly covered by particles in a given square at a certain focal depth of an image to the total area of the said square. The two types prepared with a lower mass of sorbent material had coverages of 15% and 19%, whilst those prepared with a greater mass had coverages of 68% and 82% for HLB and Carboxen®, respectively (see Table S5†). For ease of developing a classification system, the films with a lower mass of material were
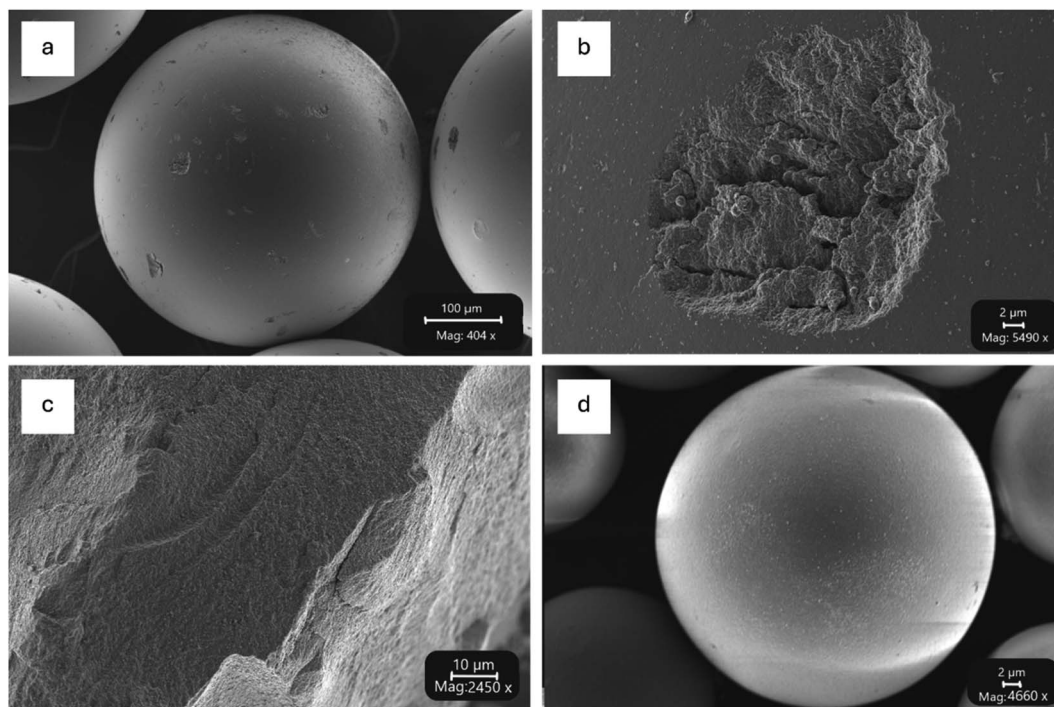
Fig. 4 SEM images of the sorbent particles. (a) Carboxen® particle. (b) Close-up of a crevice on the surface of the Carboxen® particle. (c) Close-up of the surface of a ground Carboxen® particle. (d) HLB particle.

Fig. 5 Light micrograph of the PDMS thin film.

labelled 15 (Car15 and HLB15) and those with a greater mass of material 80 (Car80 and HLB80), based on these results. Additionally, films with the sorbent material on the surface were labelled OT (CarOT and HLBOT). With these increases in the sorbent material, less light passed through the PDMS films and versions with the sorbents on the surface were opaque (Fig. 6c and f).

Film thicknesses were determined for each film type using light micrographs taken from the side of a film stuck to a glass microscope slide (see Fig. S11 in the ESI†). Dependant on the sorbent type and mass utilised, the average film thickness varied (Table 1), with the PDMS film being the thinnest. Generally, the HLB films were thinner than the Carboxen® containing films, due to the smaller particle size of the sorbent. Interestingly, the film thickness for the films prepared with Carboxen® increased from the lower mass to the larger mass, to finally the CarOT films, whereas the HLBOT films were thinner than the HLB films with a larger mass added. The relatively low

% RSDs indicate that, despite some variation, the films were uniform in their thickness.

In addition to the average film thickness, the thickened edges were measured. They were incorporated to facilitate film handling and increase the weight for submersion in samples and were found to range between 890 and 1150 μm across all film types.

Surface area analysis using BET was done for the PDMS film, as well as the films impregnated with the sorbents directly on the surface. With multi-point BET analysis, a PDMS surface area of 17.1 $m^2\,g^{-1}$ (correlation coefficient: 0.980415) was estimated, whilst surface areas of 30.5 $m^2\,g^{-1}$ (correlation coefficient: 0.999953) and 47.4 $m^2\,g^{-1}$ (correlation coefficient: 0.999914) were estimated for the thin films with Carboxen® and HLB impregnated on the surface, respectively. This increase in the surface area arises from the adsorbent particles protruding from the PDMS film surface, as well as due to the pores in the adsorbent particles themselves. The poorer correlation coefficient obtained for the PDMS film is likely due to the low mass analysed, as well as due to the fact that PDMS is an absorbent, and thus the volume of the thin film, rather than the surface area, is relevant. Moreover, the estimation of the pore size distribution and volume for the impregnated films confirmed that sorbents maintained their porous nature after addition to the films and were not negatively altered.

Analysis and comparison of thin film extraction efficiencies

From computational results and previous research (EPA Method 552.3), it has been determined that the extraction of
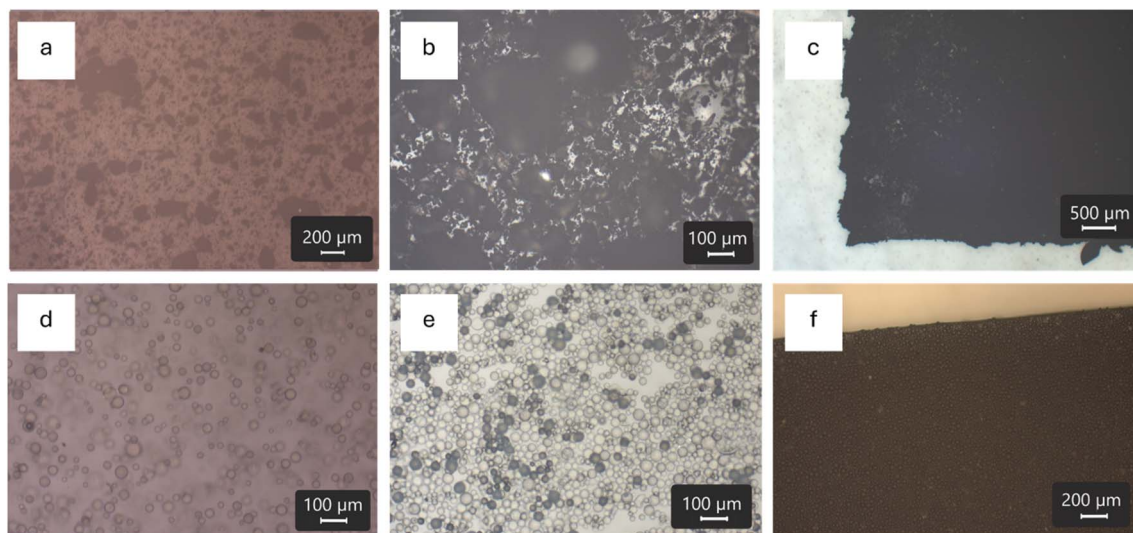
Fig. 6 Light micrographs of thin films prepared with sorbents. (a)–(c) Carboxen® impregnated PDMS films. (a) Lower mass of sorbent added. (b) Greater mass of sorbent added. (c) Sorbent on the film surface. (d)–(f) HLB impregnated PDMS films. (d) Lower mass of sorbent added. (e) Greater mass of sorbent added. (f) Sorbent on the film surface.

Table 1 Average film thickness and the corresponding standard deviation and % RSD measured from the light micrographs of the various film types

	Film type						
	PDMS	Car15	Car80	CarOT	HLB15	HLB80	HLBOT
Average thickness (μm)	241.6	320.2	435.8	468.8	279.3	385	320.5
Standard deviation	46.5	36.3	16.6	82.5	22.3	27.9	35.9
% RSD	19	11	3.8	18	8.0	7.1	11

HAAs from water is optimal when the analytes are protonated, and therefore an acidic pH is required and was applied for thin film extraction purposes. After employing EPA Method 552.3 to determine the residual analytes in solution, standardized peak area ratios were determined. The peak areas of both control types, those that were prepared and immediately stored, as well as those that were treated identically to the standards undergoing thin film extraction, were almost equal, indicating little to no analyte loss during the extraction period (Fig. 7). Numerical evaluation with ANOVA confirmed that the minor differences in the control peak areas were statistically insignificant, as all analytes, except BDCAA ($p = 0.029$), had p values larger than the critical value (see Table S6†). Consequently, any analyte changes observed between the controls and the extraction standards may be attributed to successful extraction, rather than degradation or volatilization due to time, temperature, or losses to the stirrer bar or vial walls, during extraction. Although BDCAA is known to be one of the analytes that decomposes more easily,[58] the small variance between the controls is more likely to stem from instrumental or preparative variations than decomposition. Given that the reported rate constant for BDCAA decomposition is 0.0011 day^{-1} and considering that this is even lower than those of CDBAA and TBAA,[58] which did not demonstrate a statistically significant change between the

controls, the statistical significance of BDCAA appears to point towards small changes arising from a different source than the treatment of the controls. An additional measure of quality was the excellent precision, which was reflected in the repeatability (measured as percent relative standard deviation, % RSD). Across all film types and analytes, the % RSD was well below 15%, with most being below 5%. Exceptions (one entire replicate and one analyte in a specific replicate) that exceeded 15% were tested for outliers (z-score) and were removed after confirmation.

By calculating differences between the controls and extraction standards, theoretical extraction efficiencies could be calculated as percentages (Fig. 8). Negative percentages reflect cases where the analyte peak area was higher after extraction, compared to the control. Although strictly not possible, these increases may be caused by slight variations in measurement or preparation, yet are of no great concern, given their negligible quantities.

Especially PDMS films resulted in negative or extremely low percentages, indicating that PDMS films extracted little to no analytes. Previous studies, investigating the best fiber material for HS-SPME of HAAs, found similar results, as they reported that PDMS-fibers performed among the poorest of all sorbents tested, which was attributed to the lack of pores of appropriate
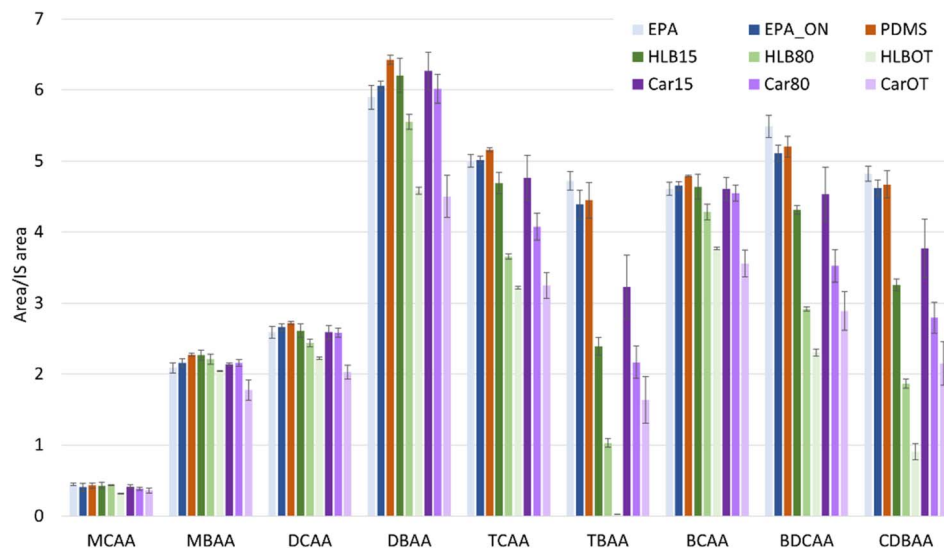
Fig. 7 Averages of triplicate area ratios of spiked deionized water, extracted with different thin film types, followed by processing and analysis with EPA Method 552.3. Outliers were determined with the z-score and error bars represent the standard deviation.

size.[16,22] In the context of the computational results presented in this study, this was unexpected, as due to the negative binding energies of the interfaces some extraction was anticipated.

However, only one PDMS monomer was modelled, and thus the steric interactions of multiple monomers in a polymeric material were not considered. Since the siloxane oxygen is between
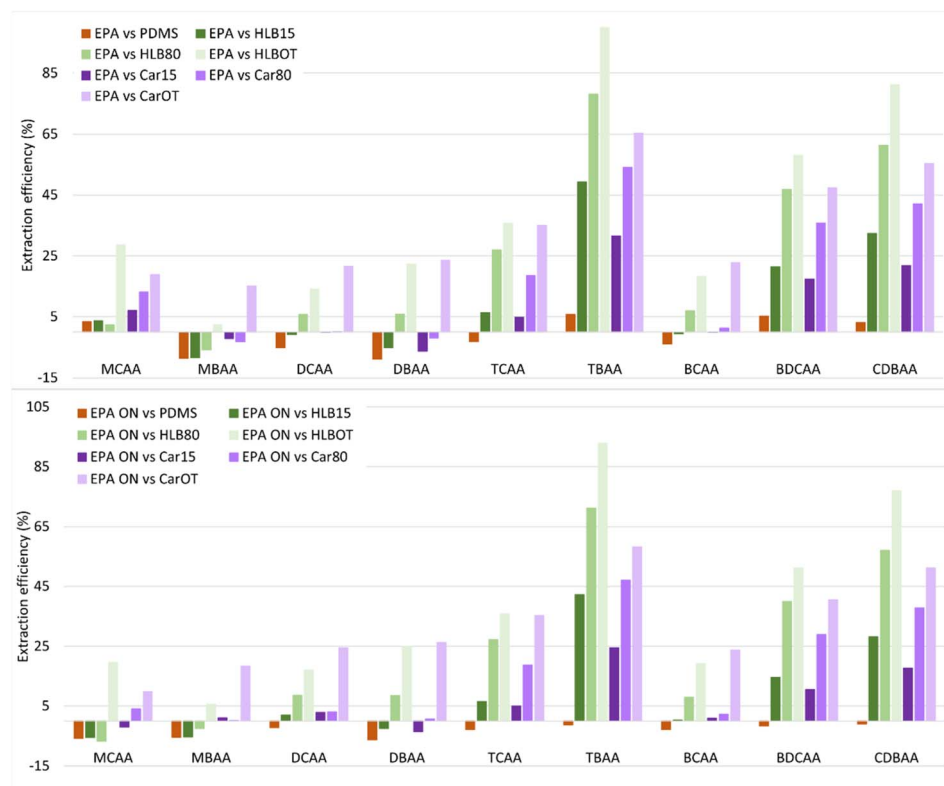

Fig. 8 Extraction efficiencies, represented as percentage reduction between the control and the extraction standards, after extraction. Note that the areas represented in Fig. 7 were used to calculate the extraction efficiencies depicted here as percentages. Outliers were tested using the z-score and removed before calculating averages. Top: the difference between a control stored in a freezer immediately after preparation and the sample containing thin films with different sorbents for 24 hours. Bottom: the difference between a control left to stand for 24 hours and the samples containing the thin films.

two methyl-silicon groups, it is less available to form hydrogen bonds with the analytes.

The addition of either sorbent to PDMS enhanced the extraction efficiencies, as reflected in the drastic decreases in peak areas observed for the majority of analytes. Only a few analytes resulted in negative extraction efficiencies, as the peak areas increased slightly (MCAA, MBAA, DBAA, and BCAA for sorbent 15 films and MCAA, MBAA, and DBAA for sorbent 80 films). This is in line with studies investigating the best fiber material for HS-SPME-based extraction of HAAs, which found that PDMS-fibers performed the weakest when compared to mixed fibers, such as Carboxen®–PDMS.[22,23] Moreover, we found that efficiencies improved substantially with an increase in the amount of sorbent added and improved even further for films with the sorbent added to the PDMS surface during curing (CarOT and HLBOT). Only MCAA and MBAA deviated from this trend, as a higher extraction efficiency was calculated for the HLB15 film compared to the HLB80 film, and for the Car15 film compared to the Car80 film, respectively. Considering that both these analytes gave the lowest instrument responses and that MCAA is notoriously difficult to detect with GC-ECD, this was unsurprising.[51]

A statistical comparison of the film types (15 vs. 80 vs. OT) within each sorbent group confirmed the significance of the observed differences in peak areas. Apart from MCAA extracted with Carboxen®, all p-values were well below the critical value and therefore the null hypothesis was rejected (Table 2). Beyond the rejection or acceptance of the null hypothesis, the p-value may provide insights into how well the data fit the null hypothesis, based on how far they deviate from the critical value.[59] Judging from the low values calculated for almost all analytes, the film types differ substantially in their extraction efficiencies. Much like the previous cases, the deviation of MCAA from the trend may be attributed to the poor sensitivity of the ECD to this compound.[51]

Tri-substituted analytes (TCAA, TBAA, BDCAA, and CDBAA) were extracted most efficiently by both sorbents (HLB and Carboxen®). Nonetheless, HLB-containing films resulted in higher extraction efficiencies for these compounds, whilst Carboxen®-containing films extracted more mono- and di-substituted analytes. This shows how the sorbents have distinct selectivity, despite the chemical properties varying very little between the analytes. It has been reported that Carboxen®–PDMS thin films better extract VVOCs, whereas HLB–PDMS films are better suited for a broader range of VOCs.[46] Although HAAs are not VOCs, a similar trend applies, as Carboxen® performed better for the analytes with lower boiling points (mono- and di-substituted). A relationship between the order of analyte substitution and extraction efficiency of films with Carboxen® on the surface was observed. For HLB, this trend was only applicable to the brominated species, as the extraction of DCAA was lower than that of both MCAA and TCAA. Moreover, the extraction efficiencies for the brominated species tended to be higher than the chlorinated species. Even in the mixed species, the extraction efficiencies followed the order: BCAA < BDCAA < CDBAA, where the dichlorinated analyte was lower than the dibrominated analyte.

In light of the computational trends and hypothesis that the electronegative halogens directly influence the hydrogen bond formation and therefore the extraction efficiency, the inter-analyte experimental results confirm this to a degree. The correlation between the levels of substitution and extraction was evident in both data sets, confirming the hypothesis. However, it was unexpected that the brominated species were extracted more efficiently. This demonstrates the predictive power of computational results as well as their shortfalls. Since computational modelling requires simplification of reality, assumptions need to be made and details omitted, leading to partial congruence between experimental and computational results. In this instance, the solvent effect is the most likely simplification that causes the discrepancy between the data sets. Regardless, the computational model accurately predicted that HLB would be the superior sorbent (compared to PDMS) and even provided valuable insight into which analytes would be extracted most efficiently. For these reasons, similar models of other sorbents could provide useful insights into which sorbents would be likely applicable for HAA extraction.

The experimental data demonstrated the great potential of thin films impregnated with Carboxen® or HLB for the extraction and/or pre-concentration of HAAs from water. Although the extraction time is longer than those of other methods, it is done at room temperature, which makes the method a facile and green alternative to methods that require elevated temperatures.[22,23] Considering that TBAA, CDBAA, and BDCAA are reportedly difficult to analyse[25,32,35,50] and that the brominated species are more cyto- and genotoxic than the chlorinated species,[12,60] the sensitivity of methods towards these analytes could be increased using HLB impregnated thin films. Moreover, the application could potentially be expanded to enhance sensitivity towards all HAAs, with thin films containing a combination of Carboxen® and HLB, since Carboxen® was more selective for mono- and di-substituted analytes.

Although methods, which achieve excellent LODs (in the ppt range) and might include simultaneous extraction and

Table 2 Summary of the p-values calculated with single factor ANOVA (95% confidence level) for nine analytes between the means of the different film types of one sorbent type (HLB or Carboxen®) to determine whether the observed differences in the extraction efficiencies are statistically significant

	MCAA	MBAA	DCAA	DBAA	TCAA	TBAA	BCAA	BDCAA	CDBAA
HLB	0.026	0.036	0.011	0.002	0.0002	2.401×10^{-5}	0.006	4.184×10^{-6}	1.794×10^{-5}
Car	0.141	0.003	0.0003	0.0003	0.0006	0.009	0.0003	0.002	0.003

derivatization[22,61] or require no preparation at all (in the case of LC-based analysis)[36,38,41] have been reported, thin film extraction represents an easy and cost-effective approach for laboratories, particularly in developing countries that might not have access to expensive equipment required for such methods.

Conclusions

In-house synthesis of PDMS thin films for the application of HAA extraction from water was successfully performed, followed by an extraction test. This method has the advantage of easy adjustment to the required film size and sorbent impregnation as desired. Moreover, successful extraction was demonstrated at room temperature, which reduces energy costs and makes the method greener than alternative methods. Extraction tests demonstrated that the addition of either Carboxen® or HLB sorbent substantially improved the extraction potential compared to PDMS-only films. Films with the sorbents on the surface proved to have the greatest extraction potential, with HLB being more selective towards tri-substituted analytes and Carboxen® towards mono- and di-substituted analytes. Furthermore, the selectivity towards the brominated species was slightly higher than that towards the chlorinated species. Considering that these types of HAAs are more prevalent in saline water,[62,63] which increasingly is desalinated to become potable water, methods sensitive towards these analytes are highly relevant. The extraction method is flexible and may be included in various combinations. For example, in conjunction with back extraction, it may be used in pre-concentration for LC-based methods or in GC-based methods for more classical extraction and desorption. The choice of the analysis and removal method may influence the reusability of the thin films; however, PDMS and the chosen sorbents are known to be very stable and robust. Trends observed in the computational data correlated well with the experimental results and could thus be used to propose hydrogen bonding, and therefore physisorption, as the basis for the extraction of analytes from water using HLB. The results show great potential for the application of thin films in the extraction of HAAs from water.

Data availability

The data supporting this article have been included as part of the ESI.†

Author contributions

Petra van der Merwe: methodology, investigation, formal analysis, and writing – original draft preparation. Patricia Forbes: conceptualization, methodology, formal analysis, writing – review & editing, supervision, resources, and funding acquisition.

Conflicts of interest

There are no conflicts to declare.

Acknowledgements

References

1 M. J. Plewa and S. D. Richardson, *J. Environ. Sci.*, 2017, **58**, 1.

2 World Health Organization, *Guidelines for drinking-water quality, Fourth edition incorporating the first and second addenda*, Geneva, 2022.

3 United States Environmental Protection Agency, *National Primary Drinking Water Regulations: Disinfectants and Disinfection Byproducts*, Federal Register, United States, 1998, vol. 63.

4 The European Parliament and the Council of the European Union, *Directive (EU) 2020/2184 of the European Parliament and of the Council of 16 December 2020 on the quality of water intended for human consumption*, European Union, 2020.

5 Water Air and Climate Change Bureau Healthy Environments and Consumer Safety Branch Health Canada, *Guidelines for Canadian Drinking Water Quality*, Guideline Technical Document, Haloacetic Acids, Health Canada, Ottawa, Canada, 2008.

6 National Health and Medical Research Council, *Australian Drinking Water Guidelines 6*, Canberra, 2011.

7 Ministry of Health Labour and Welfare Japan, *Water Quality*, 2015.

8 Ministry of Health China and Standardization Administration of China, *National Standard of the People's Republic of China*, China, 2006.

9 Department of Water Affairs and Forestry, *South African Water Quality Guidelines, Volume 1, Domestic Use*, Pretoria, South Africa, 1996.

10 T. A. Bellar, J. J. Lichtenberg and R. C. Kroner, *J. Am. Water Resour. Assoc.*, 1974, **66**, 703–706.

11 R. Sinha, A. K. Gupta and P. S. Ghosal, *J. Environ. Chem. Eng.*, 2021, **9**, 106511.

12 M. J. Plewa, J. E. Simmons, S. D. Richardson and E. D. Wagner, *Environ. Mol. Mutagen.*, 2010, **51**, 871–878.

13 National Center for Biotechnology Information, PubChem Compound Summary, PubChem Compound Summary, accessed 6 February 2024.

14 D. Benanou, F. Acobas and P. Sztajnbok, *Water Res.*, 1998, **32**, 2798–2806.

15 B. F. Scott and M. Alaee, *Water Qual. Res. J. Can.*, 1998, **33**, 279–293.

16 M. N. Sarrión, F. J. Santos and M. T. Galceran, *Anal. Chem.*, 2000, **72**, 4865–4873.

17 E. T. Urbansky, *J. Environ. Monit.*, 2000, **2**, 285–291.

18 United States Environmental Protection Agency, J. W. Hodgeson, J. Collins and R. E. Barth, *Method 552, Determination of Haloacetic Acids in Drinking Water by Liquid-Liquid Extraction, Derivatization, and Gas Chromatography with Electron Capture Detection*, 1990.

19 United States Environmental Protection Agency, J. W. Hodgeson and D. Becker, *Method 552.1, Determination of Haloacetic Acids and Dalapon in Drinking Water by Ion-Exchange Liquid-Solid Extraction and Gas Chromatography with an Electron Capture Detector, Revision 1.0*, 1992.

20 United States Environmental Protection Agency, D. J. Munch, J. W. Munch and A. M. Pawlecki, *Method 552.2, Determination of Haloacetic Acids and Dalapon in Drinking Water by Liquid-Liquid Extraction, Derivatization and Gas Chromatography with Electron Capture Detection, Revision 1.0*, 1995.

21 United States Environmental Protection Agency, M. M. Domino, B. V. Pepich, D. J. Munch, P. S. Fair and Y. Xie, *Method 552.3, Determination of Haloacetic Acids and Dalapon in Drinking Water by Liquid-Liquid Microextraction, Derivatization, and Gas Chromatography with Electron Capture Detection, Revision 1.0*, Technology Applications, Inc., 2003, vol. 552.

22 M. J. Cardador and M. Gallego, *Anal. Bioanal. Chem.*, 2010, **396**, 1331–1343.

23 M. N. Sarrion, F. J. Sanots and M. M. T. Galceran, *Anal. Chem.*, 2000, **72**, 4865–48733.

24 A. M. Casas Ferreira, M. E. Fernández Laespada, J. L. Pérez Pavón and B. Moreno Cordero, *J. Chromatogr. A*, 2013, **1318**, 35–42.

25 E. S. Franco, V. L. Pádua, M. D. V. R. Rodriguez, D. F. Silva, M. Libânio, M. C. Pereira, P. H. G. Silva, I. C. Santanta Júnior, B. A. Rocha, J. A. Camargo, A. O. Mourão and J. L. Rodrigues, *Microchem. J.*, 2019, **150**, 104088.

26 W. Li, Y. Liu, J. Duan and D. Mulcahy, *Anal. Methods*, 2013, **5**, 2258–2266.

27 W. Sadia and A. Pauzi, *Chromatographia*, 2009, **69**, 1447–1451.

28 M. Saraji and A. A. H. Bidgoli, *J. Chromatogr. A*, 2009, **1216**, 1059–1066.

29 S. Waseem and M. P. Abdullah, *J. Chromatogr. Sci.*, 2010, **48**, 188–193.

30 United States Environmental Protection Agency, A. D. Zaffiro, M. Zimmerman, B. V. Pepich, R. W. Slingsby, R. F. Jack, C. A. Pohl and D. J. Munch, *Method 557, Determination of Haloacetic Acids, Bromate, and Dalapon in Drinking Water by Ion Chromatography Electrospray Ionization Tandem Mass Spectrometry (IC-ESI-MS/MS)*, 2009.

31 A. M. Dixon, D. C. Delinsky, J. V. Bruckner, J. W. Fisher and M. G. Bartlett, *J. Liq. Chromatogr. Relat. Technol.*, 2004, **27**, 2343–2355.

32 B. Huang and J. Rohrer, *J. Chromatogr. A*, 2020, **1630**, 461538.

33 L. Ranjbar, A. J. Gaudry, M. C. Breadmore and R. A. Shellie, *Anal. Chem.*, 2015, **87**, 8673–8678.

34 X. Zhang, C. Saini, C. Pohl and Y. Liu, *J. Chromatogr. A*, 2020, **1621**, 461052.

35 M. C. Prieto-Blanco, M. F. Alpendurada, P. López-Mahía, S. Muniategui-Lorenzo, D. Prada-Rodríguez, S. MacHado and C. Gonçalves, *Talanta*, 2012, **94**, 90–98.

36 C. Planas, Ó. Palacios, F. Ventura, M. R Boleda, J. Martín and J. Caixach, *Anal. Bioanal. Chem.*, 2019, **411**, 3905–3917.

37 D. Kou, X. Wang and S. Mitra, *J. Chromatogr. A*, 2004, **1055**, 63–69.

38 B. Lajin and W. Goessler, *Anal. Chem.*, 2020, **92**, 9156–9163.

39 L. Meng, S. Wu, F. Ma, A. Jia and J. Hu, *J. Chromatogr. A*, 2010, **1217**, 4873–4876.

40 C.-Y. Chen, S.-N. Chang and G.-S. Wang, *J. Chromatogr. Sci.*, 2009, **47**, 67–74.

41 A. C. B. Berrio, S. C. Barbosa, J. L. O. Arias, L. C. Marcolin and E. G. Primel, *J. Braz. Chem. Soc.*, 2022, **33**, 281–290.

42 P. Varanusupakul, N. Vora-adisak and B. Pulpoka, *Anal. Chim. Acta*, 2007, **598**, 82–86.

43 J. B. Wilcockson and F. A. P. C. Gobas, *Environ. Sci. Technol.*, 2001, **35**, 1425–1431.

44 S. Seidi, M. Tajik, M. Baharfar and M. Rezezadeh, *TrAC, Trends Anal. Chem.*, 2019, **118**, 810–827.

45 I. Bruheim, X. Liu and J. Pawliszyn, *Anal. Chem.*, 2003, **75**, 1002–1010.

46 N. C. Kfoury, J. A. Whitecavage and J. R. Stuff, *Comparison of Three Types of Thin Film-Solid Phase Microextraction Phases for Beverage Extractions*, 2021.

47 K. Murtada, V. Galpin, J. J. Grandy, V. Singh, F. Sanchez and J. Pawliszyn, *Sustainable Chem. Pharm.*, 2021, **21**, 100435.

48 J. J. Grandy, E. Boyaci and J. Pawliszyn, *Anal. Chem.*, 2016, **88**, 1760–1767.

49 J. J. Grandy, V. Singh, M. Lashgari, M. Gauthier and J. Pawliszyn, *Anal. Chem.*, 2018, **90**, 14072–14080.

50 M. J. Cardador and M. Gallego, *J. Chromatogr. A*, 2014, **1340**, 15–23.

51 Y. Xie, *Water Res.*, 2001, **35**, 1599–1602.

52 C. A. Schneider, W. S. Rasband and K. W. Eliceiri, *Nat. Methods*, 2012, **9**, 671–675.

53 J. Tomasi, B. Mennucci and R. Cammi, *Chem. Rev.*, 2005, **105**, 2999–3094.

54 M. J. Frisch, G. W. Trucks, H. B. Schlegel, G. E. Scuseria, M. A. Robb, J. R. Cheeseman, G. Scalmani, V. Barone, G. A. Petersson, H. Nakatsuji, X. Li, M. Caricato, A. V. Marenich, J. Bloino, B. G. Janesko, R. Gomperts, B. Mennucci, H. P. Hratchian, J. V. Ortiz, A. F. Izmaylov, J. L. Sonnenberg, D. Williams-Young, F. Ding, F. Lipparini, F. Egidi, J. Goings, B. Peng, A. Petrone, T. Henderson, D. Ranasinghe, V. G. Zakrzewski, J. Gao, N. Rega, G. Zheng, W. Liang, M. Hada, M. Ehara, K. Toyota, R. Fukuda, J. Hasegawa, M. Ishida, T. Nakajima, Y. Honda, O. Kitao, H. Nakai, T. Vreven, K. Throssell, J. A. Montgomery Jr, J. E. Peralta, F. Ogliaro, M. J. Bearpark, J. J. Heyd, E. N. Brothers, K. N. Kudin, V. N. Staroverov, T. A. Keith, R. Kobayashi, J. Normand, K. Raghavachari, A. P. Rendell, J. C. Burant, S. S. Iyengar, J. Tomasi, M. Cossi, J. M. Millam, M. Klene, C. Adamo, R. Cammi, J. W. Ochterski, R. L. Martin, K. Morokuma, O. Farkas, J. B. Foresman and D. J. Fox, *GaussView 5.0*, Gaussian, Inc., Wallingford, CT, E.U.A., 2016.

55 E. Arunan, G. R. Desiraju, R. A. Klein, J. Sadlej, S. Scheiner, I. Alkorta, D. C. Clary, R. H. Crabtree, J. J. Dannenber, P. Hobza, H. G. Kjaergaard, A. C. Legon, B. Mennucci and D. J. Nesbitt, *Pure Appl. Chem.*, 2011, **83**, 1637–1641.

56 S. J. Grabowski, in *Understanding Hydrogen Bonds - Theoretical and Experimental Views*, Royal Society of Chemistry (RSC), 2021, pp. 1–40.

57 J. Abrahamson, *Carboxen® Synthetic Carbon Adsorbents for Industrial Water Purification*, 2021.

58 X. Zhang and R. A. Minear, *Water Res.*, 2002, **36**, 3665–3673.

59 G. Di Leo and F. Sardanelli, *European Radiology Experimental*, 2020, **4**, 1–8.

60 L. Zhang, L. Xu, Q. Zeng, S. H. Zhang, H. Xie, A. L. Liu and W. Q. Lu, *Mutat. Res., Genet. Toxicol. Environ. Mutagen.*, 2012, **741**, 89–94.

61 M. J. Cardador, A. Serrano and M. Gallego, *J. Chromatogr. A*, 2008, **1209**, 61–69.

62 E. C. Ged and T. H. Boyer, *Desalination*, 2014, **345**, 85–93.

63 T. Manasfi, M. De Méo, B. Coulomb, C. Di Giorgio and J. L. Boudenne, *Environ. Int.*, 2016, **88**, 94–102.